

## Chemical analysis of surface oxygenated moieties of fluorescent carbon nanoparticles

Jie Huang,<sup>†ab</sup> Christopher P. Deming,<sup>†a</sup> Yang Song,<sup>a</sup> Xiongwu Kang,<sup>a</sup> Zhi-You Zhou<sup>a</sup> and Shaowei Chen<sup>\*a</sup>

Received 8th November 2011, Accepted 8th December 2011

DOI: 10.1039/c2nr11689h

Water-soluble carbon nanoparticles were prepared by refluxing natural gas soot in concentrated nitric acid. The surface of the resulting nanoparticles was found to be decorated with a variety of oxygenated species, as suggested by spectroscopic measurements. Back potentiometric titration of the nanoparticles was employed to quantify the coverage of carboxylic, lactonic, and phenolic moieties on the particle surface by taking advantage of their vast difference of acidity ( $pK_a$ ). The results were largely consistent with those reported in previous studies with other carbonaceous (nano)materials. Additionally, the presence of *ortho*- and *para*-quinone moieties on the nanoparticle surface was confirmed by selective labelling with *o*-phenylenediamine, as manifested in X-ray photoelectron spectroscopy, photoluminescence, and electrochemical measurements. The results further supported the arguments that the surface functional moieties that were analogous to 9,10-phenanthrenequinone were responsible for the unique photoluminescence of the nanoparticles and the emission might be regulated by surface charge state, as facilitated by the conjugated graphitic core matrix.

### Introduction

Carbon-based (nano)materials have been widely used in many important scientific and technological applications, for instance, as atomic scale probes, hydrogen storage matrices, chemical sensors, solar cells, and drug delivery vehicles, primarily because of their unique optical and electronic properties as well as overall chemical inertness, low costs, and relative ease of preparation.<sup>1–14</sup> Among these, carbon nanoparticles (CNPs) represent a unique addition to the family of functional carbon nanomaterials. Whereas the surface structures of carbon nanoparticles are not as well-defined as their well-known cousins, fullerenes and carbon nanotubes, it is generally found that the nanoparticle cores are of graphitic nature and the rich chemistry of the nanoparticle surface renders them to behave as a unique platform for more complicated chemical functionalization and hence for diverse applications.<sup>11,15–20</sup> So far, a number of effective synthetic procedures have been reported for the preparation of carbon nanoparticles. For instance, Hu *et al.*<sup>8</sup> synthesized photoluminescent carbon nanoparticles of 3 nm in diameter by laser irradiation of a suspension of carbon powders in an organic solvent. Sun and coworkers<sup>18</sup> demonstrated that carbon nanoparticles might be produced by laser ablation of a carbon target in the presence of water vapour with argon as the carrier gas, and

subsequent surface passivation with simple organic ligands rendered the particles to emit strong photoluminescence. Li *et al.*<sup>21</sup> described a one-step synthesis of water-soluble carbon nanoparticles based on alkali- or acid-assisted ultrasonic treatments of glucose and the resulting particles emitted apparent photoluminescence. Carbon nanoparticles have also been prepared by electrochemical treatments of multiwall carbon nanotubes, as demonstrated by Zhou and coworkers<sup>14,19</sup> where carbon nanoparticles of spherical shape and narrow size distribution ( $2.8 \pm 0.5$  nm in diameter) were formed. More recently, a very simple and yet effective synthetic protocol was reported for the preparation of multicolor luminescent carbon nanoparticles by acid refluxing of the combustion soot of candles<sup>22</sup> and natural gas.<sup>23</sup> FTIR and <sup>13</sup>C NMR spectroscopic studies showed that the nanoparticle surface was covered with a variety of oxygen-containing groups such as carboxylic acid and quinone moieties.<sup>23</sup> Notably, the resulting nanoparticles exhibited interesting electrochemical characteristics which were ascribed to functional derivatives on the nanoparticle surface that are analogous to, for instance, 9,10-phenanthrenequinone; and the nanoparticle photoluminescence was found to enhance markedly by a simple hydrothermal treatment or by the addition of strong reducing agents such as NaBH<sub>4</sub>.<sup>24</sup> This was most likely due to the reduction of the quinone derivatives, leading to increased intensity of the  $\pi$ - $\pi^*$  transitions.<sup>25</sup>

Despite the progress, the fundamental mechanism of the carbon nanoparticle photoluminescence remains largely unknown, primarily because of the lack of understanding of the molecular structures of the nanoparticle surface. This is the primary motivation of the present study. In this article, we

<sup>a</sup>Department of Chemistry and Biochemistry, University of California, Santa Cruz, California, 95064, USA. E-mail: shaowei@ucsc.edu

<sup>b</sup>Department of Chemical Engineering, Northwest University, Xi'an, Shaanxi, 710069, China

<sup>†</sup> These authors contributed equally to this work.

carried out two sets of studies to elucidate the chemical functional moieties on the carbon nanoparticle surface. The first involves acid–base titration to identify and quantify several oxygenated functional groups. Specifically, the oxygenated species such as carboxyl groups, cyclic anhydrides, lactones, and hydroxyl groups of phenolic character, as depicted in Scheme 1, may be differentiated and quantified by neutralization with  $\text{NaHCO}_3$ ,  $\text{Na}_2\text{CO}_3$ , and  $\text{NaOH}$ , respectively, by taking advantage of the large discrepancy of their acidity ( $\text{p}K_{\text{a}}$ ).<sup>26,27</sup> In the second study, selective chemical labelling will be employed to confirm the presence of *ortho*- and *para*-quinone moieties on the nanoparticle surface by using *o*-phenylenediamine as the molecular probe,<sup>28,29</sup> as manifested in electrochemical and spectroscopic measurements.

## Experimental section

### Chemicals

Nitric acid ( $\text{HNO}_3$ , 69.8%, Fisher), sodium hydroxide ( $\text{NaOH}$ , 99%, Aldrich), sodium carbonate ( $\text{Na}_2\text{CO}_3$ , 99%, Aldrich), sodium bicarbonate ( $\text{NaHCO}_3$ , 99%, Aldrich), hydrochloric acid (37.1%, Fisher), and *o*-phenylenediamine ( $\geq 98.0\%$ , Sigma-Aldrich) were all used as received. Water was supplied by a Barnstead Nanopure Water System ( $18.3 \text{ M}\Omega \cdot \text{cm}$ ).

### Synthesis of carbon nanoparticles

The synthetic procedure of fluorescent carbon nanoparticles has been described previously.<sup>23,24,30</sup> Briefly, carbon soot was collected on the inside wall of a glass beaker by placing the beaker upside-down above the flame of a natural gas burner. Typically 100 mg of the soot was then refluxed in 10 mL of 5 M  $\text{HNO}_3$  for 12 h. When cooled down to room temperature, the brownish yellow supernatant after centrifugation was neutralized by  $\text{Na}_2\text{CO}_3$  and then dialyzed against Nanopure water through a dialysis membrane for 3 days, affording purified carbon nanoparticles, which exhibited well-defined graphitic crystalline lattices with an average diameter of  $4.8 \pm 0.6 \text{ nm}$ , as determined by (high-resolution) transmission electron microscopic measurements.<sup>23,24,30</sup>

### Back potentiometric titration

Experimentally, a calculated amount of the carbon nanoparticles was mixed with a base solution, and the excess was determined by back potentiometric titration with  $\text{HCl}$  by following a literature procedure.<sup>27</sup> Briefly, carbon nanoparticles (4 mL,  $9.3 \mu\text{M}$ ) dissolved in Nanopure water were mixed with 4 mL of 0.025

N  $\text{NaOH}$ , 0.050 N  $\text{Na}_2\text{CO}_3$ , or 0.022 N  $\text{NaHCO}_3$  for 12 h under continuous stirring. The excessive base was then quantified by back titration with a 0.112 N  $\text{HCl}$  solution, and the solution pH was monitored by a Corning 445 pH meter. Control experiments were also carried out by titrating the respective base solution (4 mL) of  $\text{NaOH}$ ,  $\text{Na}_2\text{CO}_3$ , or  $\text{NaHCO}_3$  with the same  $\text{HCl}$  solution. The difference of the  $\text{HCl}$  volumes at the equivalence points between these two titration curves was then used for the quantitative assessments of the acid moieties on the carbon nanoparticle surface.

### Chemical labelling

The experiment was carried out by following a literature procedure.<sup>20</sup> Briefly, 25 mg of the carbon nanoparticles were dissolved in 7 mL of glacial acetic acid at  $40^\circ\text{C}$ ; and separately, 11 mg of the labelling compound, *o*-phenylenediamine, was dissolved in 10 mL of ethanol to make a 1 mM solution. One mL of the labelling solution was then mixed with the carbon nanoparticles under magnetic stirring for half an hour at  $100^\circ\text{C}$ . After being cooled to room temperature, the product was purified by dialysis to remove the solvents and excessive labelling compound. The resulting labelled nanoparticles remained soluble in water.

### Spectroscopies

UV-vis spectra were acquired with an ATI Unicam UV4 spectrometer, and photoluminescence measurements were carried out with a PTI fluorescence spectrometer by using the same solution as those for UV-vis studies. X-ray photoelectron spectra (XPS) were recorded with a PHI 5400/XPS instrument equipped with an  $\text{Al K}_{\alpha}$  source operated at 350 W and at  $10^{-9}$  torr. Silicon wafers were sputtered by argon ions to remove carbon from the background and used as substrates. The spectra were charge-referenced to the  $\text{Au } 4f_{7/2}$  peak (83.8 eV) of sputtered gold.

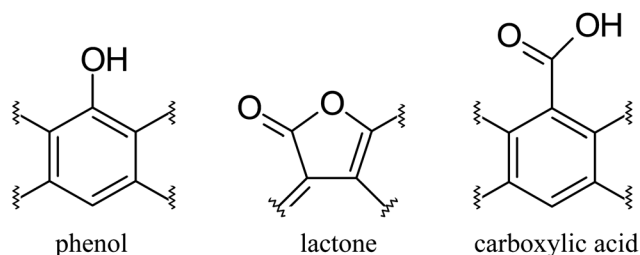
### Electrochemistry

Voltammetric measurements were carried out with a CHI 440 electrochemical workstation. A glassy carbon electrode (diameter 3 mm, from Bioanalytical Systems, Inc) was used as the working electrode. A  $\text{Ag}/\text{AgCl}$  wire and a Pt coil were used as the reference and counter electrode, respectively. The electrolyte solutions were deaerated with ultrahigh-purity  $\text{N}_2$  for 10 min before the acquisition of electrochemical data, and the electrolyte solution was blanketed with a nitrogen atmosphere during the entire experimental procedure.

## Results and discussion

### Back potentiometric titration

As mentioned above, the carbon nanoparticles were produced by refluxing natural gas soot in concentrated  $\text{HNO}_3$ , and hence exhibited varied oxygenated species on the particle surface that most likely included carboxylic, lactonic, and phenolic moieties, as suggested in varied spectroscopic measurements.<sup>23,24,30</sup> As the acidity of the carboxylic, lactone, and phenol groups (Scheme 1) differ over several orders of magnitude with the respective  $\text{p}K_{\text{a}}$  at  $\sim 4.0$ , 8.2, and 10.0,<sup>31</sup> there is a marked discrepancy of their



**Scheme 1** Structures of phenolic, lactonic and carboxylic moieties.

reactivity towards base neutralization. Specifically, weak base  $\text{NaHCO}_3$  can only neutralize the most acidic carboxylic groups, whereas both carboxylic and lactonic groups can be neutralized by the somewhat stronger base of  $\text{Na}_2\text{CO}_3$ ; and for the even stronger base of  $\text{NaOH}$ , the total acidity of phenolic, lactonic, carboxylic groups can be determined. Therefore, by three separate titration measurements of the same sample, the concentration of each acidic group can be quantified. In fact, this unique chemistry has been exploited for the quantitative determination of acid functional groups on varied carbon surfaces.<sup>26,32</sup>

In the present study, carbon nanoparticles were first mixed with a calculated amount of base, and the excessive base was then back titrated by using a  $\text{HCl}$  solution. Fig. 1 (dashed curves) depicts the titration curves of carbon nanoparticles (4 mL, 9.3  $\mu\text{M}$ ) with  $\text{HCl}$  (0.112 N) after the addition of 4 mL of different base solutions: (A)  $\text{NaOH}$  (0.025 N), (B)  $\text{Na}_2\text{CO}_3$  (0.050 N), and (C)  $\text{NaHCO}_3$  (0.022 N). The titration curves (solid curves) of

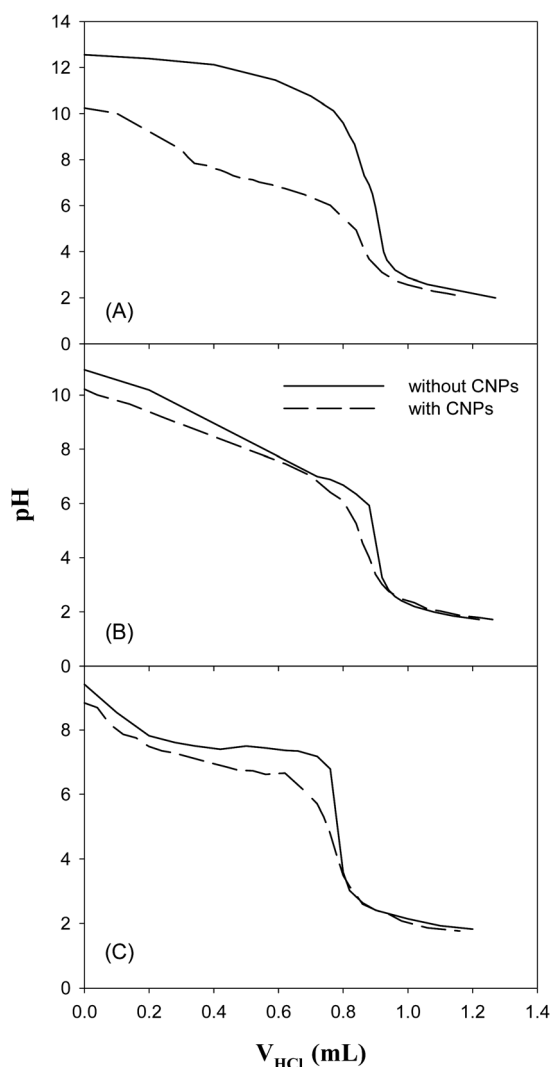


**Fig. 1** Titration curves (dashed) of carbon nanoparticle solutions (4 mL, 9.3  $\mu\text{M}$ ) with  $\text{HCl}$  (0.112 N) after the addition of 4 mL of base solutions: (A)  $\text{NaOH}$  (0.025 N), (B)  $\text{Na}_2\text{CO}_3$  (0.050 N), and (C)  $\text{NaHCO}_3$  (0.022 N). The control experiments of titrations with the corresponding blank base solutions (4 mL) were also included as the solid curves.

a same amount of the blank base solutions with the same  $\text{HCl}$  solution were also included. The difference between the  $\text{HCl}$  volumes at the equivalence points ( $\Delta V_{\text{HCl}}$ ) in each base solution was used to quantify the concentration of acidic groups on the carbon nanoparticle surface. It can be seen that in the three base titrations, with the addition of increasing amounts of  $\text{HCl}$ , the solution pH decreases accordingly, where the equivalence points were well-defined by the abrupt decrease of the solution pH with the addition of about 0.8 to 1.0 mL of  $\text{HCl}$ . Table 1 summarizes the  $\text{HCl}$  volume and solution pH at the equivalence point in each titration, from which the number of acidic functional groups on the carbon nanoparticle surface was determined. For instance, it can be seen that based on the titration with  $\text{NaHCO}_3$ , there were approximately 33.0 carboxylic acid groups on the carbon nanoparticle surface; and the combined number of the lactonic and carboxylic groups was determined to be 49.6 by titration analysis with  $\text{Na}_2\text{CO}_3$ . Further analysis with  $\text{NaOH}$  titration showed that the total number of the acidic groups (including carboxylic, lactonic and phenolic groups) was 91.3. That is, there are on average 33.0, 16.6, and 41.7 carboxylic, lactonic, and phenolic groups on the carbon nanoparticle surface. Note that the surface coverage of the carboxylic moieties ( $4.2 \times 10^{13}/\text{cm}^2$ , Table 1) is very comparable to that ( $1.05 \times 10^{13}/\text{cm}^2$ ) reported with ACF 25 carbon fibres as determined by similar Boehm titration,<sup>32</sup> but at least an order of magnitude higher than that observed with multiwalled carbon nanotubes as determined by electrochemical measurements.<sup>20,33</sup> These results are consistent with the water solubility and spectroscopic data of the carbon nanoparticles.<sup>23,24</sup>

Interestingly, the photoluminescence (PL) of the carbon nanoparticles exhibited an apparent variation with solution pH. Fig. 2 shows the excitation and emission spectra of the nanoparticles in water at different solution pH as adjusted by (A)  $\text{NaOH}$ , (B)  $\text{Na}_2\text{CO}_3$ , and (C)  $\text{NaHCO}_3$ . It can be seen that whereas the changing trend of the PL intensity with solution pH was not well-defined, (after being normalized with the respective absorbance by UV-vis measurements, not shown), the peak positions of both the excitation and emission spectra actually exhibited an apparent blue shift with increasing solution pH, regardless of the specific base used in adjusting the solution acidity, as manifested in panel (D). For instance, in the titration by  $\text{NaOH}$ , the excitation and emission peak positions of the nanoparticles in solution were found to shift by about 20 nm from  $\lambda_{\text{ex}} = 344$  nm and  $\lambda_{\text{em}} = 437$  nm at pH = 3.69 to  $\lambda_{\text{ex}} = 322$  nm and  $\lambda_{\text{em}} = 420$  nm at pH = 10.25. Similar variations can also be seen with the other two bases ( $\text{Na}_2\text{CO}_3$  and  $\text{NaHCO}_3$ ). One may note that in the previous study with much smaller carbon nanoparticles (dia. 1 nm)<sup>22</sup> the PL peak positions also exhibited a similar blue shift with increasing solution pH, although no mechanistic interpretation was included. Taken together, these observations suggest that (i) the photoluminescent moieties most likely resided on the nanoparticle surface (*vide infra*),<sup>23,24</sup> and (ii) the negative charge on the nanoparticle surface increased the HOMO–LUMO energy gap of the photoactive moieties. In a previous study,<sup>34</sup> Zhang *et al.* carried out theoretical studies based on density functional theory to examine the effects of aromatic substituent groups on the electronic structures and spectral properties of a rhenium complex and found that electron-donating groups increased the LUMO energy and hence the LUMO–HOMO gap, leading to a blue shift of the absorption

**Table 1** Summary of surface concentrations of acidic moieties on carbon nanoparticle surface as determined by titration measurements (Fig. 1)

Base	Without CNPs		With CNPs		$\Delta V_{\text{HCl}}$ (mL)	Functional Groups	Number per particle	Surface coverage ( $10^{13}/\text{cm}^2$ )
	$V_{\text{HCl}}$ (mL)	pH	$V_{\text{HCl}}$ (mL)	pH				
NaOH	0.8753	7.00	0.8451	4.70	0.0302	carboxylic, lactonic, and phenolic	91.33	11.63
$\text{Na}_2\text{CO}_3$	0.9065	3.78	0.8901	3.82	0.0164	lactonic and carboxylic	49.60	6.32
$\text{NaHCO}_3$	0.7806	5.10	0.7697	4.47	0.0109	carboxylic	32.96	4.20

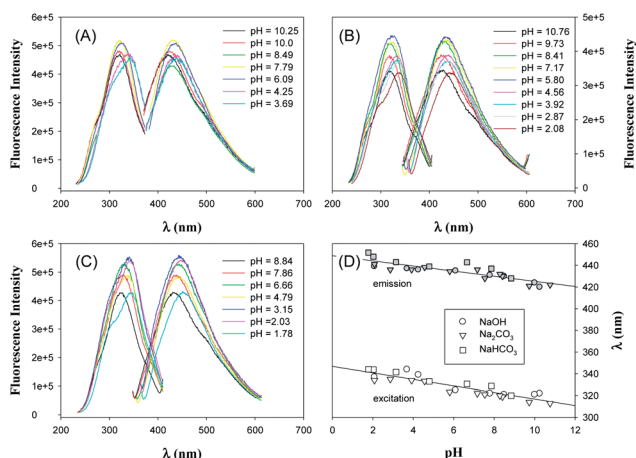


**Fig. 2** Photoluminescence spectra of carbon nanoparticles at different pH which was adjusted by the addition of a HCl solution into the particle solution with excessive bases: (A) NaOH, (B)  $\text{Na}_2\text{CO}_3$ , and (C)  $\text{NaHCO}_3$ . The solutions were the same as those in Fig. 1. Panel (D) depicts the variation of the excitation and emission peak positions with solution pH as adjusted by different bases. The data points are acquired from panels (A)–(C).

spectra. Therefore, the sensitive regulation of the carbon nanoparticle photoluminescence by solution pH (and hence surface negative charge from the deprotonation of the nanoparticle surface acid groups, Table 1) is most likely facilitated by the conjugated network afforded by the nanoparticle graphitic matrix.<sup>23</sup>

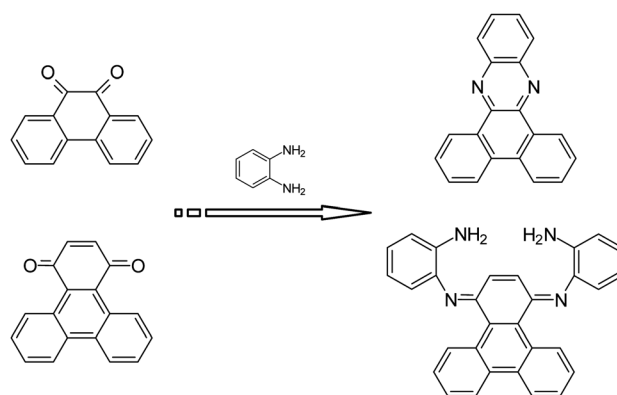
### Surface labelling by o-phenylenediamine

It should be noted that the above titration studies are mostly confined to acidic functional groups that may be readily deprotonated by the added bases. Other oxygenated species, such as quinone derivatives that are presumably responsible for the electrochemical and photoluminescence characteristics,<sup>23,24</sup> will have to be identified in a different manner. In the present study, the presence of quinone moieties on the carbon nanoparticle surface was confirmed by using o-phenylenediamine as the molecular probe. This is to take advantage of the specific reactivity of o-phenylenediamine towards *ortho*- and *para*-quinones forming imine adducts (Scheme 2), whereas no reaction is anticipated with other oxygen-containing groups such as carboxylic acid or carbonyl groups.<sup>28</sup>

The successful labelling of the carbon nanoparticles was first manifested in XPS measurements. Fig. 3 shows the XPS survey spectra of the original and labelled carbon nanoparticles within the range of 0 to 1100 eV. In both samples, a prominent peak

centered at 287.0 eV appears. Note that this binding energy is greater than the typical values for the 1s electrons of  $\text{sp}^2$  hybridized (graphitic) carbon<sup>35–39</sup> but is consistent with that for carbonyl carbon.<sup>40</sup> The asymmetrical shape of the peak suggests that it actually entails contributions from these different carbons. Another peak emerges at 534.0 eV, which may be ascribed to the oxygen 1s electrons in C=O and C–O–C.<sup>40</sup> Additionally, after the nanoparticles were labelled with o-phenylenediamine, the peak for nitrogen 1s electrons appears and centers around 400.7 eV, as shown in the figure inset of a high-resolution survey scan within the range of 395 eV to 405 eV. These observations further confirm the presence of quinone groups on the nanoparticle surface which were successfully labelled by o-phenylenediamine<sup>23</sup> (additional evidence was observed in FTIR measurements where the labelled nanoparticles exhibited a new band at  $1600\text{ cm}^{-1}$  that might be ascribed to the C=N vibration and another at  $3536\text{ cm}^{-1}$  to the N–H moiety, as compared to the unlabelled carbon nanoparticles<sup>41</sup>). However, the low signal intensity renders it difficult to differentiate and quantify the *ortho*- and *para*-quinone moieties, although in previous studies with other carbonaceous materials such as graphite and glassy carbon powders that underwent similar chemical labelling, both *ortho*- and *para*-quinone moieties could be identified in XPS measurements.<sup>28</sup>

Consistent results were obtained in electrochemical measurements. Fig. 4 shows the differential pulse voltammograms (DPVs) of the carbon nanoparticles before and after the labelling reactions within the potential range of +0.8 to –0.8 V. It can be seen that in contrast to the original particles that showed a largely featureless profile, the labelled nanoparticles exhibited a new (and broad) pair of voltammetric peaks ( $I_a/I_c$ ) with the formal potential at around 0 V. This feature may be attributed to



**Scheme 2** Selective Labelling of *ortho*- and *para*-Quinones by o-Phenylenediamine.

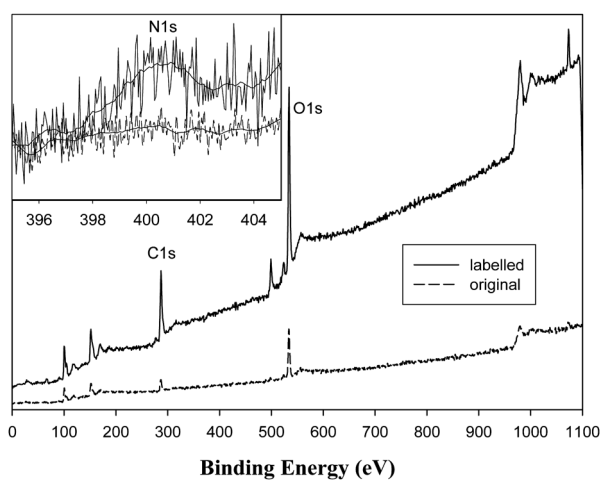


**Fig. 3** XPS survey spectra of the carbon nanoparticles before (dashed curve) and after (solid curve) labelling with *o*-phenylenediamine. Inset shows the magnified portion between 395 and 405 eV, where lines are the smoothing curves of the experimental data.

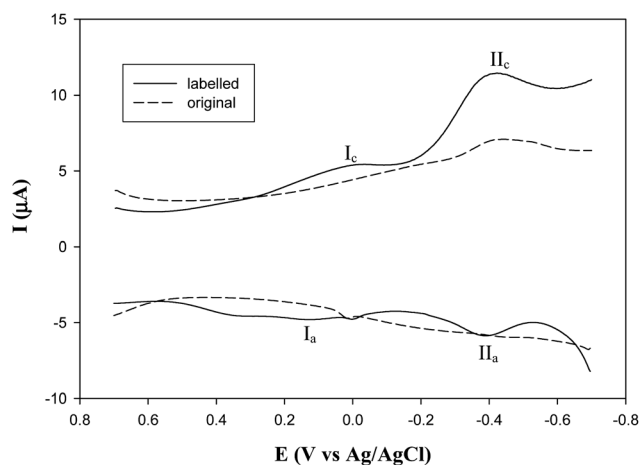


**Fig. 4** Differential pulse voltammograms of the carbon nanoparticles before (dashed curve) and after (solid curve) labelling with *o*-phenylenediamine at a glassy carbon electrode (dia. 3 mm) in 0.1 M KCl solution. Nanoparticle concentration was about 10 mg mL<sup>-1</sup>. DC potential sweep rate 10 mV s<sup>-1</sup>, and pulse amplitude 50 mV.

the 2-proton, 2-electron redox reaction of the phenazine-like structure formed in the labelling of *ortho*-quinones (Scheme 2).<sup>28</sup> Additionally, another pair of voltammetric peaks (II<sub>a</sub>/II<sub>c</sub>) can be seen for the labelled sample at around -0.40 V, whereas for the original nanoparticles, only a much smaller cathodic peak appeared at *ca.* -0.43 V but without a well-defined anodic wave. This is most likely due to the redox reaction of the imine structure formed in the labelling of *para*-quinone by *o*-phenylenediamine (Scheme 2).<sup>28</sup> The appearance of these two voltammetric features suggests that both *ortho*- and *para*-quinone moieties were indeed present on the carbon nanoparticle surface.

Interestingly, after labelling with *o*-phenylenediamine, the carbon nanoparticles exhibited an apparent difference in their photoluminescence characteristics. Fig. 5 depicts the excitation and emission spectra of both the original (dashed curves) and

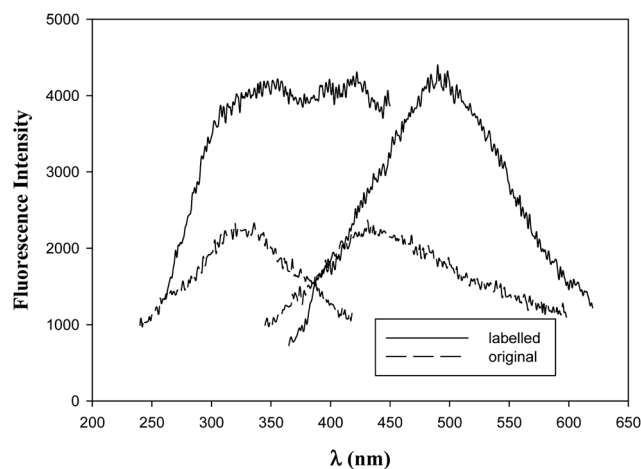


**Fig. 5** Excitation and emission spectra of the carbon nanoparticles before (dashed curves) and after (solid curves) labelling with *o*-phenylenediamine. Particle concentration was about 1 mg mL<sup>-1</sup>.

labelled (solid curves) nanoparticles. It can be seen that the original nanoparticles showed a well-defined excitation peak at 327 nm and an equally prominent emission peak at 430 nm.<sup>23</sup> Yet, after labelling with *o*-phenylenediamine, both the excitation and emission peak positions exhibited a marked red shift. For instance, the emission peak is now located at 490 nm and at least four main peaks can be deconvoluted in the excitation spectrum at 307 nm, 355 nm, 399 nm, and 425 nm. These new photoluminescence behaviours may be attributed to the formation of the phenazine-like structure upon the labelling of the *ortho*-quinone moieties by *o*-phenylenediamine (Scheme 2), as phenazine derivatives are known to emit fluorescence in the yellow-green region and feature apparent absorption peaks within the range of 300 and 500 nm.<sup>42-44</sup> Importantly, the obvious discrepancy of the nanoparticle photoluminescence upon *o*-phenylenediamine labelling also confirms the hypothesis that the phenanthrenequinone moieties are indeed the photoactive moieties responsible for the photoemission activity of the carbon nanoparticles.<sup>23</sup>

## Conclusion

In this study, acid groups on the carbon nanoparticle surface were identified and quantified by back potentiometric titration with varied bases. This was to exploit the large discrepancy of the p*K*<sub>a</sub> between the carboxylic, lactonic and phenolic groups and hence their different reactivity towards base neutralization. The results based on titration analysis showed the carbon nanoparticles possessed a surface coverage of carboxylic groups that was comparable to those reported previously for other carbonaceous (nano)materials. In addition, the presence of quinone groups on the nanoparticle surface was confirmed by the selective labelling with *o*-phenylenediamine, as manifested by spectroscopic and electrochemical measurements. Taken together, these results support the argument that the nanoparticle surface was indeed decorated with a wide variety of oxo functional moieties which included quinone derivatives that gave rise to the unique photoluminescence of the nanoparticles.

## Acknowledgements

This work was supported, in part, by the National Science Foundation (CHE-1012256 and DMR-0804049) and by the ACS-Petroleum Research Fund (49137-ND10). J.H. was supported, in part, by a research fellowship from the China Scholarship Council. XPS work was performed as a User Project at the Molecular Foundry, Lawrence Berkeley National Laboratory, which is supported by the US Department of Energy.

## Notes and references

- 1 P. Avouris, *Chem. Phys.*, 2002, **281**, 429.
- 2 T. W. Ebbesen, K. Tanigaki and S. Kuroshima, *Chem. Phys. Lett.*, 1991, **181**, 501.
- 3 S. B. Zhu, T. G. Xu, H. B. Fu, J. C. Zhao and Y. F. Zhu, *Environ. Sci. Technol.*, 2007, **41**, 6234.
- 4 Y. Saito and S. Uemura, *Carbon*, 2000, **38**, 169.
- 5 N. Hamada, S. Sawada and A. Oshiyama, *Phys. Rev. Lett.*, 1992, **68**, 1579.
- 6 S. J. Tans, M. H. Devoret, H. J. Dai, A. Thess, R. E. Smalley, L. J. Geerligs and C. Dekker, *Nature*, 1997, **386**, 474.
- 7 S. J. Yu, M. W. Kang, H. C. Chang, K. M. Chen and Y. C. Yu, *J. Am. Chem. Soc.*, 2005, **127**, 17604.
- 8 S. L. Hu, K. Y. Niu, J. Sun, J. Yang, N. Q. Zhao and X. W. Du, *J. Mater. Chem.*, 2009, **19**, 484.
- 9 X. L. Kong, L. C. L. Huang, C. M. Hsu, W. H. Chen, C. C. Han and H. C. Chang, *Anal. Chem.*, 2005, **77**, 259.
- 10 K. Ushizawa, Y. Sato, T. Mitsumori, T. Machinami, T. Ueda and T. Ando, *Chem. Phys. Lett.*, 2002, **351**, 105.
- 11 L. Cao, X. Wang, M. J. Meziani, F. S. Lu, H. F. Wang, P. J. G. Luo, Y. Lin, B. A. Harruff, L. M. Veca, D. Murray, S. Y. Xie and Y. P. Sun, *J. Am. Chem. Soc.*, 2007, **129**, 11318.
- 12 X. L. Kong, L. C. L. Huang, S. C. V. Liao, C. C. Han and H. C. Chang, *Anal. Chem.*, 2005, **77**, 4273.
- 13 Y. D. Glinka, K. W. Lin, H. C. Chang and S. H. Lin, *J. Phys. Chem. B*, 1999, **103**, 4251.
- 14 B.-P. Qi, Y.-M. Long, L. Bao, C. Liu, Z.-L. Zhang and D.-W. Pang, *Journal of Electrochemistry*, 2011, **17**, 271.
- 15 A. B. Bourlinos, A. Stassinopoulos, D. Anglos, R. Zboril, V. Georgakilas and E. P. Giannelis, *Chem. Mater.*, 2008, **20**, 4539.
- 16 Q. L. Zhao, Z. L. Zhang, B. H. Huang, J. Peng, M. Zhang and D. W. Pang, *Chem. Commun.*, 2008, 5116.
- 17 B. R. Selvi, D. Jagadeesan, B. S. Suma, G. Nagashankar, M. Arif, K. Balasubramanyam, M. Eswaramoorthy and T. K. Kundu, *Nano Lett.*, 2008, **8**, 3182.
- 18 Y. P. Sun, B. Zhou, Y. Lin, W. Wang, K. A. S. Fernando, P. Pathak, M. J. Meziani, B. A. Harruff, X. Wang, H. F. Wang, P. J. G. Luo, H. Yang, M. E. Kose, B. L. Chen, L. M. Veca and S. Y. Xie, *J. Am. Chem. Soc.*, 2006, **128**, 7756.
- 19 J. G. Zhou, C. Booker, R. Y. Li, X. T. Zhou, T. K. Sham, X. L. Sun and Z. F. Ding, *J. Am. Chem. Soc.*, 2007, **129**, 744.
- 20 G. G. Wildgoose, P. Abiman and R. G. Compton, *J. Mater. Chem.*, 2009, **19**, 4875.
- 21 H. T. Li, X. D. He, Y. Liu, H. Huang, S. Y. Lian, S. T. Lee and Z. H. Kang, *Carbon*, 2011, **49**, 605.
- 22 H. P. Liu, T. Ye and C. D. Mao, *Angew. Chem., Int. Ed.*, 2007, **46**, 6473.
- 23 L. Tian, D. Ghosh, W. Chen, S. Pradhan, X. J. Chang and S. W. Chen, *Chem. Mater.*, 2009, **21**, 2803.
- 24 L. Tian, Y. Song, X. J. Chang and S. W. Chen, *Scr. Mater.*, 2010, **62**, 883.
- 25 R. M. Cory and D. M. McKnight, *Environ. Sci. Technol.*, 2005, **39**, 8142.
- 26 H. P. Boehm, *Carbon*, 1994, **32**, 759.
- 27 H. P. Boehm, *Carbon*, 2002, **40**, 145.
- 28 C. A. Thorogood, G. G. Wildgoose, A. Crossley, R. M. J. Jacobs, J. H. Jones and R. G. Compton, *Chem. Mater.*, 2007, **19**, 4964.
- 29 C. A. Thorogood, G. G. Wildgoose, J. H. Jones and R. G. Compton, *New J. Chem.*, 2007, **31**, 958.
- 30 Y. Song, X. W. Kang, N. B. Zuckerman, B. Phebus, J. P. Konopelski and S. W. Chen, *Nanoscale*, 2011, **3**, 1984.
- 31 C. A. Leon y Leon and L. R. Radovic, *Chemistry and Physics of Carbon*, 1994, **24**, 213.
- 32 X. Feng, N. Dementev, W. G. Feng, R. Vidic and E. Borguet, *Carbon*, 2006, **44**, 1203.
- 33 A. T. Masheter, L. Xiao, G. G. Wildgoose, A. Crossley, H. J. C. John and R. G. Compton, *J. Mater. Chem.*, 2007, **17**, 3515.
- 34 T. T. Zhang, J. F. Jia and H. S. Wu, *J. Phys. Chem. A*, 2010, **114**, 12251.
- 35 M. Rybachuk and J. M. Bell, *Carbon*, 2009, **47**, 2481.
- 36 S. Turgeon and R. W. Paynter, *Thin Solid Films*, 2001, **394**, 44.
- 37 U. Dettlaff-Weglikowska, J. M. Benoit, P. W. Chiu, R. Graupner, S. Lebedkin and S. Roth, *Curr. Appl. Phys.*, 2002, **2**, 497.
- 38 G. Iucci, V. Carravetta, P. Altamura, M. V. Russo, G. Paolucci, A. Goldoni and G. Polzonetti, *Chem. Phys.*, 2004, **302**, 43.
- 39 K. Siegbahn, *Philos. Trans. R. Soc. London, Ser. A*, 1970, **268**, 33.
- 40 X. G. Li, K. L. Huang, S. Q. Liu, N. Tan and L. Q. Chen, *Trans. Nonferrous Met. Soc. China*, 2007, **17**, 195.
- 41 M. A. Fryling, J. Zhao and R. L. McCreery, *Anal. Chem.*, 1995, **67**, 967.
- 42 J. H. Zhu, J. A. Olmstead and D. G. Gray, *J. Wood Chem. Technol.*, 1995, **15**, 43.
- 43 V. Zozulya, Y. Blagoi, G. Lober, I. Voloshin, S. Winter, V. Makitruk and A. Shalamay, *Biophys. Chem.*, 1997, **65**, 55.
- 44 C. E. M. Carvalho, I. M. Brinn, A. V. Pinto and M. D. F. R. Pinto, *J. Photochem. Photobiol., A*, 2000, **136**, 25.